Transport in Porous Media (2021) 136:521–539
https://doi.org/10.1007/s11242-020-01523-9

Darcy–Carreau Model and Nonlinear Natural Convection for Pseudoplastic and Dilatant Fluids in Porous Media

Pedro Vayssière Brandão[1] · Mohamed Najib Ouarzazi[2]

Received: 5 June 2020 / Accepted: 25 November 2020 / Published online: 3 January 2021

Abstract
The linear and weakly nonlinear stability analyses are carried out to study instabilities in Darcy–Bénard convection for non-Newtonian inelastic fluids. The rheological model considered here is the Darcy–Carreau model, which is an extension to porous media of Carreau rheological model usually used in clear fluid media. The linear stability approach showed that the critical Rayleigh number and wave number corresponding to the onset of convection are the same as for Newtonian fluids. By employing weakly nonlinear theory, we derived a cubic Landau equation that describes the temporal evolution of the amplitude of convection rolls in the unstable regime. It is found that the bifurcation from the conduction state to convection rolls is always supercritical for dilatant fluids. For pseudoplastic fluids, however, the interplay between the macroscale properties of the porous media and the rheological characteristics of the fluid determines the supercritical or subcritical nature of the bifurcation. In the parameter range where the bifurcation is supercritical, we determined and discussed the combined effects of the fluid properties and the porous medium characteristics on the amplitude of convection rolls and the corresponding average heat transfer for both pseudoplastic and dilatant fluids. Remarkably, we found that the curves describing these effects collapse onto the universal curve for Newtonian fluids, provided the average apparent viscosity is used to define Rayleigh number.

Keywords Natural convection · Porous media · Darcy–Carreau model · Weakly nonlinear stability

1 Introduction

Natural convection in a porous medium saturated by a Newtonian fluid induced by heating from below is a thermal instability problem that has been extensively investigated in the past due to its major importance in many problems that appear in nature and engineering

✉ Mohamed Najib Ouarzazi
mohamed-najib.ouarzazi@univ-lille.fr

[1] Department of Industrial Engineering, Alma Mater Studiorum Università di Bologna, Viale Risorgimento 2, 40136 Bologna, Italy

[2] Unité de Mécanique de Lille, Joseph Boussinesq, EA 7512, Université de Lille, Bd. Paul Langevin, 59655 Villeneuve d'Ascq Cedex, France

applications (for detailed reviews, see Nield and Bejan 2017). The instability of the conduction state occurs as a result of the buoyancy effect due to heating. Supercritical stationary bifurcation takes place when the Rayleigh number, which is a dimensionless measure of the temperature difference across the layer, exceeds a critical value.

Recently, there has been an increasing interest on the corresponding problem for non-Newtonian fluids. For a viscoelastic fluid confined in a porous medium heated from below, Kim et al. (2003) and Yoon et al. (2004) performed a linear stability analysis by using the modified Darcy's law based on the Oldroyd-B model. They showed that in viscoelastic fluids, such as polymeric liquids, a Hopf bifurcation as well as a stationary bifurcation may occur at the onset of convection depending on the magnitude of the viscoelastic parameters. In the case of a Hopf bifurcation, the question of whether standing or traveling waves are preferred at onset has been fully addressed by Hirata et al. (2015). The dynamics associated with the nonlinear interaction between the two kinds of instabilities, namely stationary and oscillatory instabilities, is analyzed by Taleb et al. (2016) in the framework of a weakly nonlinear theory and with two-dimensional numerical simulations. From the experimental point of view, the oscillatory character of the instability at the onset of convection was confirmed by Kolodner (1998) using DNA suspensions in clear fluid media.

For non-Newtonian visco-inelastic fluids, the rheological model usually employed is the power law model. In porous media, this model considers the drag term in Darcy's law as $\frac{\mu_a}{K}\,\mathbf{V}^*$, where $\mathbf{V}^*$ is the seepage velocity, K is the permeability of the porous medium and μ_a is the apparent viscosity given by

$$\mu_a = \eta_{ef}\,|\mathbf{V}^*|^{n-1} \tag{1}$$

where η_{ef} [Pa s^n m^{1-n}] is the effective consistency factor and n is the flow behavior index. An important deficiency of this model is that, in the limit of a vanishing $\mathbf{V}^*$, it gives infinite μ_a for shear-thinning fluids ($n < 1$) and zero apparent viscosity for shear-thickening fluids ($n > 1$). To overcome these singularities, (Nield 2011a, b) suggested a modified drag term, $\frac{\mu_0}{K}\left(1 + C\,|\mathbf{V}^*|^{n-1}\right) V^*$, i.e., a modified apparent viscosity,

$$\mu_a = \mu_0\left(1 + C\,|\mathbf{V}^*|^{n-1}\right) \tag{2}$$

where C [m^{1-n} s^{n-1}] is a constant.

According to this model, for small values of $\mathbf{V}^*$ and for $n > 1$, the drag is linear in $\mathbf{V}^*$, and one recovers the usual linear Darcy's law with μ_0 as the fluid viscosity at $\mathbf{V}^* = 0$. Consequently, as pointed out by Nield (2011a), Nield (2011b), the critical Rayleigh number at the onset of convection is independent of the power law index and, hence, equal to the one for Newtonian fluids, i.e., $Ra_c = 4\pi^2$. On the other hand, for pseudoplastic fluids ($n < 1$), the apparent viscosity μ_a becomes infinite in the limit of vanishing V^* and the approach described by Nield (2011a), Nield (2011b) cannot draw any conclusions about the onset of the instability.

In order to investigate this matter further, Barletta and Nield (2011) investigated the onset of mixed convection of both pseudoplastic and dilatant fluids in a porous layer heated from below in the presence of a horizontal throughflow. This introduces a Péclet number Pe characterizing the flow, and the Darcy–Bénard problem is recovered in the limit of zero Pe. In this limit, the linear stability results showed that Ra_c tends to infinity for shear-thinning fluids and tends to zero for shear-thickening fluids. We note that these results were obtained in the framework of the power law model which, as pointed out above, presents a singularity as the seepage velocity becomes small.

Because thermal instabilities in porous media and in a fluid clear of solid material are qualitatively similar in a number of aspects, it is interesting to recall some existing results in the literature obtained for non-Newtonian Rayleigh–Bénard problem. For shear-thinning fluids described by a power law model, Tien et al. (1969) indicated that the linear marginal stability curve cannot be determined, because of the unphysical infinite viscosity, at zero shear rate, introduced by the rheological model. Bouteraa et al. (2015) conducted a weakly nonlinear stability analysis for Rayleigh–Bénard problem in the case of pseudoplastic fluids using a Carreau rheological model. They derived a Landau amplitude equation and found that the bifurcation may be supercritical or subcritical depending on the degree of shear-thinning. The competition between rolls, squares and hexagons is also investigated (Bouteraa et al. 2015). It shows that only rolls are stable near the supercritical onset. The supercritical/subcritical nature of the bifurcation predicted by weakly nonlinear theory (Bouteraa et al. 2015) were confirmed by two-dimensional numerical simulations of the fully nonlinear problem by Jenny et al. (2015) and by Benouared et al. (2014). Although quite rare, experimental investigations of this thermal instability for shear-thinning fluids also exist. Darbouli et al. (2016) conducted experiments with Xanthan-gum solutions at different concentrations. They concluded that the onset of convection for all the concentrations used occurred around the Rayleigh value $Ra_c = 1800$, which corresponds to the Newtonian limit. This experimental result is in excellent agreement with the linear stability predictions reported by Liang and Acrivos (1970), when the Carreau rheological model is employed. This short overview indicates that the use of the power law model with small values of the seepage velocity in porous media, or weak shear rate in a clear fluid medium, becomes questionable. Since this is the case at the onset of convection, this model should be modified.

The objective of this paper is to present some new results obtained by weakly nonlinear stability theory in Darcy–Bénard convection for pseudoplastic and dilatant fluids. The analysis is conducted using a new model that extends the Carreau model to porous media. This article is organized as follows. In Sect. 2, the rheological model and the mathematical formulation of the current problem are presented. A weakly nonlinear analysis is performed in Sect. 3, which includes the derivation of the amplitude equation, results about the nature of bifurcations, the equilibrium amplitude of finite disturbances and the average heat transfer. The results based on the average apparent viscosity are presented in Sect. 3.4. Conclusions and future work are given in Sect. 4.

2 Rheological Model and Dimensionless Equations

2.1 Rheological Model

To overcome the singularity associated with shear-thinning fluids ($n < 1$) at zero shear rate in a fluid medium, a regularized form of the power law model is used. Known as the Carreau model (Carreau 1972), it is given by

$$\frac{\mu - \mu_\infty}{\mu_0 - \mu_\infty} = \left(1 + (\lambda^* \dot{\gamma})^2\right)^{\frac{n-1}{2}} \tag{3}$$

where $\dot{\gamma}$ is the shear rate, the constant μ_∞ is the infinite shear rate viscosity and λ^* is a characteristic time for the non-Newtonian fluid, defined as

$$\lambda^* = \left(\frac{\eta}{\mu_0}\right)^{\frac{1}{n-1}} \tag{4}$$

where η [Pa s^n] is the consistency factor.

Usually, μ_∞ is negligible and the Carreau model reduces to

$$\frac{\mu}{\mu_0} = \left(1 + (\lambda^* \dot{\gamma})^2\right)^{\frac{n-1}{2}} \tag{5}$$

In similar way, the singularities of the power law model associated with a porous medium can be avoided in the limit of zero filtration velocity $\mathbf{V}^*$ by adopting the following proposed rheological model, named here the Darcy–Carreau model,

$$\frac{\mu_a}{\mu_0} = \left(1 + \left(\frac{\eta_{ef}}{\mu_0}\right)^{\frac{2}{n-1}} |\mathbf{V}^*|^2\right)^{\frac{n-1}{2}} \tag{6}$$

noting that, in the limit of large $|\mathbf{V}^*|$, the power law model (1) is recovered, while the apparent viscosity takes a finite nonzero value $\mu_a = \mu_0$ in the limit of a vanishing seepage velocity $|\mathbf{V}^*|$ independent of n. In the present study, the following expression for η_{ef}, used by many authors (see Pascal and Pascal 1997 and Longo et al. 2013 for instance), is employed

$$\eta_{ef} = \eta f_p \, (\Phi K)^{\frac{1-n}{2}} \tag{7}$$

with $f_p = 8^{(-\frac{n+1}{2})} \, 2 \, (\frac{3n+1}{n})^n$ and where Φ is the porosity of the porous medium.

Introducing the characteristic time λ^* of the non-Newtonian fluid defined by (4), the Darcy–Carreau model (6) becomes

$$\frac{\mu_a}{\mu_0} = \left[1 + \left(\lambda^* f_p^{\frac{1}{n-1}} \, (\Phi K)^{-\frac{1}{2}} \, |\mathbf{V}^*|\right)^2\right]^{\frac{n-1}{2}} \tag{8}$$

In a review of non-Newtonian flow through porous media, Savins (1969) studied the effect of the tortuosity of the porous medium on the shear rate $\dot{\gamma}_p^*$ which is proportional to $(\Phi K)^{\frac{-1}{2}} \, |\mathbf{V}^*|$. Longo et al. (2013) investigated non-Newtonian axisymmetric porous gravity currents and showed that choosing the correct shear rate range for the determination of the rheological parameters is crucial for obtaining a good agreement between theory and experiments. Here we define the porous shear rate as,

$$\dot{\gamma}_p^* = f_p^{\frac{1}{n-1}} \, (\Phi K)^{\frac{-1}{2}} \, |\mathbf{V}^*| \tag{9}$$

and, hence, Eq. (8) may be written as

$$\frac{\mu_a}{\mu_0} = \left(1 + (\lambda^* \dot{\gamma}_p^*)^2\right)^{\frac{n-1}{2}} \tag{10}$$

The above form of Darcy-Carreau model looks like the Carreau model for a non-Newtonian fluid clear of solid material (5) if one assumes that the infinite shear rate viscosity μ_∞ is zero.

2.2 Mathematical Formulation

Let us consider an isotropic and homogeneous porous cavity of height H and infinite extension in the horizontal plane saturated by either a pseudoplastic fluid or a dilatant fluid. The porous medium is heated from the bottom and cooled from the top. The upper and lower horizontal walls are considered impermeable and are kept at constant temperatures T_1^* and T_0^*, respectively. We assume that the Oberbeck–Boussinesq approximation holds. The rheological model used for the apparent viscosity is supposed to obey the Darcy–Carreau rheological model (8). The equations for continuity, apparent viscosity, momentum and energy can then be written as:

$$\nabla \cdot \mathbf{V}^* = 0 \tag{11}$$

$$\frac{\mu_a}{\mu_0} = \left(1 + (\lambda^* f_p^{\frac{1}{n-1}} (\Phi K)^{\frac{-1}{2}} |\mathbf{V}^*|)^2\right)^{\frac{n-1}{2}} \tag{12}$$

$$\frac{\mu_a}{K} \mathbf{V}^* + \boldsymbol{\nabla} P^* - \rho_0 \beta (T^* - T_1^*) \mathbf{g} = 0 \tag{13}$$

$$(\rho c)_m \frac{\partial T^*}{\partial t^*} + (\rho c)_f \mathbf{V}^* \cdot \nabla T^* = k_m \nabla^2 T^* \tag{14}$$

The boundary conditions at the impermeable perfectly conducting horizontal walls are:

$$\begin{array}{l} T^* = T_0^* \quad \text{at} \quad z^* = 0 \quad \text{and} \quad T^* = T_1^* \quad \text{at} \quad z^* = H \\ W^* = 0 \quad \text{at} \quad z^* = 0, H \end{array} \tag{15}$$

where $\mathbf{V}^* = (u^*, v^*, w^*)$ is the velocity field, T^* is the temperature field, P^* is the hydrostatic pressure field, μ_a is the apparent dynamic viscosity, μ_0 is the dynamic viscosity at the zero shear rate, k_m is the effective thermal conductivity, β is the fluid thermal expansion coefficient, K is the permeability, ρ is the fluid density, $(\rho c)_m$ and $(\rho c)_f$ are the heat capacity per unit volume of the medium and the heat capacity per unit volume of the fluid, respectively. $\mathbf{g} = -g\mathbf{e_z}$ is the gravitational acceleration, with g denoting its modulus and $\mathbf{e_z}$ the unit vector along the z-axis.

We choose H, $k_m/(H(\rho c)_f)$, $H^2(\rho c)_m/k_m$, $k_m\mu_0/(K(\rho c)_f)$ and $\Delta T^* = T_0^* - T_1^*$, as reference quantities for length, velocity, time, pressure and temperature $(T^* - T_1^*)$. With this scaling, the following set of dimensionless equations is obtained:

$$\nabla \cdot \mathbf{V} = 0 \tag{16}$$

$$\left(1 + \alpha |\mathbf{V}|^2\right)^{\frac{n-1}{2}} \mathbf{V} + \boldsymbol{\nabla} P - Ra\, T\, \mathbf{e_z} = 0 \tag{17}$$

$$\frac{\partial T}{\partial t} + \mathbf{V} \cdot \nabla T - \nabla^2 T = 0 \tag{18}$$

with

$$Ra = \frac{KHg\beta\Delta T^*}{\kappa_m \mu_0} \tag{19}$$

and

$$\alpha = \lambda^{*2} f_p^{\frac{2}{n-1}} \frac{1}{\Phi K} \left(\frac{\kappa_m}{H}\right)^2, \tag{20}$$

where $\kappa_m = \frac{k_m}{(\rho c)_f}$ is the thermal diffusivity of the porous medium. If we introduce the dimensionless characteristic time of the fluid $\lambda = \frac{\lambda^*}{H^2/\kappa_m}$ and the Darcy number $Da = \frac{K}{H^2}$, equation (20) can be written as,

$$\alpha = \lambda^2 f_p^{\frac{2}{n-1}} \frac{1}{\Phi Da}, \tag{21}$$

the dimensionless boundary conditions become

$$\begin{aligned} &T = 1 \quad \text{at} \quad z = 0 \quad \text{and} \quad T = 0 \quad \text{at} \quad z = 1 \\ &W = 0 \quad \text{at} \quad z = 0, 1 \end{aligned} \tag{22}$$

and the basic state can be written in dimensionless form as

$$T_{(b)} = 1 - z \tag{23}$$

$$\boldsymbol{\nabla} P_{(b)} = +Ra\, T_{(b)}\, \mathbf{e_z} \tag{24}$$

3 Weakly Nonlinear Analysis

3.1 Derivation of Amplitude Equation

To investigate the nonlinear stability of the conductive state, infinitesimal two-dimensional perturbations are superimposed onto the basic solution:

$$\mathbf{V} = \mathbf{0} + \mathbf{v}(x, z, t), \quad T = T_{(b)} + \theta(x, z, t), \quad P = P_{(b)} + p(x, z, t) \tag{25}$$

Substituting equations (25) into (16)–(18), eliminating the pressure field and introducing the perturbation stream function ψ defined by

$$u = \frac{\partial \psi}{\partial z} \quad \text{and} \quad w = -\frac{\partial \psi}{\partial x} \tag{26}$$

leads to a set of two coupled nonlinear equations involving ψ and the temperature perturbation θ,

$$\nabla^2 \psi + Ra \frac{\partial \theta}{\partial x} = NL \tag{27}$$

$$\frac{\partial \theta}{\partial t} + \frac{\partial \psi}{\partial x} - \nabla^2 \theta = -(\mathbf{u} \cdot \nabla)\theta \tag{28}$$

where the nonlinear term NL is

$$\begin{aligned} NL = & -\alpha(n-1)\left[\left(\frac{\partial\psi}{\partial z}\right)^2\frac{\partial^2\psi}{\partial z^2}+\left(\frac{\partial\psi}{\partial x}\right)^2\frac{\partial^2\psi}{\partial x^2}\right. \\ & \left. +2\frac{\partial\psi}{\partial z}\frac{\partial\psi}{\partial x}\frac{\partial^2\psi}{\partial x\partial z}+\frac{1}{2}\left(\left(\frac{\partial\psi}{\partial z}\right)^2+\left(\frac{\partial\psi}{\partial x}\right)^2\right)\left(\frac{\partial^2\psi}{\partial x^2}+\frac{\partial^2\psi}{\partial z^2}\right)\right] \end{aligned} \tag{29}$$

The following weakly nonlinear approach is similar to the one used in Newell and Whitehead (1969) and in more recent papers in Bouteraa et al. (2015) and Requilé et al. (2020). The governing equations may be rewritten in the compact notation

$$(L'\partial_t + L(Ra))V = N. \tag{30}$$

where the vector $V = (\psi, \theta)^T$ contains the perturbation stream function and temperature. L' and L are the linear operators

$$L' = \begin{pmatrix} 0 & 0 \\ 0 & 1 \end{pmatrix} \tag{31}$$

and

$$L = \begin{pmatrix} \left(\frac{\partial^2}{\partial x^2}+\frac{\partial^2}{\partial z^2}\right) & Ra\frac{\partial}{\partial x} \\ \frac{\partial}{\partial x} & -\left(\frac{\partial^2}{\partial x^2}+\frac{\partial^2}{\partial z^2}\right) \end{pmatrix} \tag{32}$$

where N is the nonlinear operator. Above linear threshold, we introduce a small parameter ϵ which measures the distance to criticality by setting $Ra = Ra_c + \epsilon^2 R_2$, where R_2 is of order unity. This fixes the temporal scaling to

$$t_2 = \epsilon^2 t, \tag{33}$$

allowing the temporal derivative to be replaced by

$$\frac{\partial}{\partial t} \rightarrow \frac{\partial}{\partial t} + \epsilon^2\frac{\partial}{\partial t_2}. \tag{34}$$

and the evolution equations to be obtained by expanding the vector V in power series of ϵ, i.e.,

$$V = \epsilon V_1 + \epsilon^2 V_2 + \cdots \tag{35}$$

where the functions V_i depend on the slow variable t_2. By substituting (35) in the system (30), and then collecting coefficients of like powers of ϵ, the following equations are obtained;

$$(L'\partial_t + L_0)V_1 = 0, \tag{36}$$

$$(L'\partial_t + L_0)V_2 = N_{(2)} = RH_2, \tag{37}$$

$$(L^{'}\partial_t + L_0)V_3 = -L_2V_1 - L^{'}\partial_{t_2}V_1 + N_{(3)} = RH_3. \tag{38}$$

with L_0 defined as the linear operator for $Ra = Ra_c$, and RH_n representing the final right-hand terms, while L_2 is given by

$$L_2 = \begin{pmatrix} 0 & R_2\frac{\partial}{\partial x} \\ 0 & 0 \end{pmatrix}. \tag{39}$$

First-order variables $\tilde{V}_1 = \left(\psi_1, \theta_1\right)^T$ are expanded in normal modes,

$$\left(\psi_1, \theta_1\right) = A(t_2)\left(\Psi_1, \Theta_1\right)e^{ik_c x + \sigma t}\sin(\pi z) + \ c.c \tag{40}$$

where A is the amplitude of the disturbances, which depends on the slow time t_2, σ is the temporal growth rate of the instability and c. c stands for complex conjugate. Inserting (40) into (36) leads to the dispersion relation,

$$\sigma = -(k^2 + \pi^2) + \frac{k^2}{(k^2 + \pi^2)}Ra \tag{41}$$

The neutral stability condition is found by setting $\sigma = 0$ which leads to $Ra = (k^2 + \pi^2)^2/k^2$. The minimum Ra and its corresponding k are $Ra_c = 4\pi^2$ and $k_c = \pi$. As it is well known, these critical values are associated with Darcy–Bénard convection for Newtonian fluids. This means that the non-Newtonian nature of the fluid has no effects on linear characteristics of the instability, as it was predicted by Nield (2011a), Nield (2011b) for dilatant fluids. With the use of Darcy–Carreau model, this result also holds for pseudo-plastic fluids.

On the other hand, $\partial\sigma/\partial Ra = 1/2$ at (Ra_c, k_c), meaning that the Taylor series expansion for σ in the vicinity of Ra_c, assuming an unchanged wavenumber $k = k_c$, can be written as

$$\sigma(Ra) = \sigma(Ra = Ra_c) + (1/2)(Ra - Ra_c) + \cdots \tag{42}$$

with $\sigma(Ra = Ra_c) = 0$. This relation states that the linear growth rate of the instability in the vicinity of critical conditions is $(1/2)(Ra - Ra_c)$, which justifies the introduction of the slow time scale t_2 defined by (33).

The eigenfunctions at $O(\epsilon)$ and $O(\epsilon^2)$ are, respectively,

$$\left(\theta_1, \psi_1\right) = (1, 2\pi i)A(t_2)\,e^{ik_c x}\sin(\pi z) + \ c.c, \tag{43}$$

$$\theta_2 = -\pi \mid A \mid^2 \sin(2\pi z) \quad \text{and} \quad \psi_2 = 0, \tag{44}$$

where the quantity θ_2 represents a nonlinear correction to the conductive basic temperature and is generated by the interaction of the fundamental mode with its complex conjugate.

After inserting V_1 and V_2 into the third-order equation (38), there is no need to solve this equation. Projecting the whole equation onto $V^{\dagger}$ instead, where $V^{\dagger}$ is the solution of the adjoint linear problem yields a solvability condition, known as the Fredholm alternative. We apply the solvability condition using the inner product,

$$\left\langle V_i, V_j \right\rangle = \frac{1}{2\pi/k_c}\int_0^{2\pi/k_c}\int_0^1 V_i \cdot V_j^* \mathrm{d}z\,\mathrm{d}y, \tag{45}$$

where V_j^* is the complex conjugate of V_j. Re-introducing the original variables $t = t_2/\varepsilon^2$, this solvability condition yields the amplitude equation

$$\frac{dA}{dt} = \beta A - \delta A |A|^2. \tag{46}$$

where the explicit expressions for the coefficients appearing in (46) are:

$$\beta = \frac{R_a - Ra_c}{2} \quad \text{and} \quad \delta = 2\pi^4 + 10\pi^6 \alpha (n-1) \tag{47}$$

with β representing the linear growth rate of the instability, determined above by a linear stability analysis, and δ is the Landau constant.

3.2 Supercritical/Subcritical Nature of Bifurcations

The Landau constant δ in the amplitude equation (46) contains two different nonlinear contributions present in the current problem. The first one, i.e., $2\pi^4$, models the nonlinear thermal advection, while the second one, i.e., $10\pi^6 \alpha (n-1)$, models the non-Newtonian character of the fluid. Physically, the latter can be related to the variation in the apparent viscosity $\mu_a = (1 + (\alpha |\mathbf{V}|)^2)^{(n-1)/2}$ near the onset of convection,

$$\frac{d\mu_a}{d|\boldsymbol{V}|^2} (|\boldsymbol{V}|^2 = 0) = \alpha \frac{n-1}{2} \tag{48}$$

The above equation states that in the vicinity of the convection state threshold, where $|\boldsymbol{V}|$ is small, the nonlinear correction decreases the apparent viscosity for pseudoplastic fluids ($n < 1$), while the opposite occurs for dilatant fluids ($n > 1$). If we introduce the parameter

$$\alpha_p = \alpha \left| \frac{n-1}{2} \right| = \left| \frac{n-1}{2} \right| f_p^{\frac{2}{n-1}} \lambda^2 \frac{1}{\Phi Da} \tag{49}$$

that may be considered as a measure of non-Newtonian effects, then the Landau constant may be written as $\delta = 2\pi^4 \pm 20\pi^6 \alpha_p$. The $+$ and $-$ signs correspond, respectively, to dilatant and pseudoplastic fluids.

The sign of the Landau constant δ determines whether or not we are dealing with a subcritical bifurcation. The nonlinear coefficient δ is always positive for Newtonian ($n = 1$) as well as dilatant fluids ($n > 1$), while its sign may be positive or negative for pseudoplastic fluids ($n < 1$). For Darcy–Bénard convection of Newtonian fluids we retrieve the well-known result that the first bifurcation is supercritical. For non-Newtonian fluids, we conclude that the bifurcation is always supercritical for dilatant fluids. In the case of pseudoplastic fluids, there exists a particular value α_p^{tr} of the dimensionless number α_p related to a tricritical bifurcation point,

$$\alpha_p^{tr} = \frac{1}{10\pi^2} \tag{50}$$

such that the bifurcation from conduction to convection is supercritical when $\alpha_p < \alpha_p^{tr}$ and subcritical otherwise.

Bouteraa et al. (2015) performed a weakly nonlinear stability analysis of the respective Rayleigh–Bénard convection without porous materials in the case of pseudoplastic fluids. They found that the bifurcation from the conduction state to convection rolls may be supercritical or subcritical depending on the degree of the shear-thinning of the fluid. On the other hand, in Darcy–Bénard convection, the intrinsic properties of the porous medium, namely the Darcy number and the porosity of the porous medium, act in concert with the fluid properties to trigger the transition from supercritical to subcritical bifurcation. In fact, introducing the definition of α given by (21), the condition required for subcritical bifurcation reads,

$$\frac{\lambda^2}{\phi Da}(1-n)f_p^{\frac{2}{n-1}} > \frac{1}{5\pi^2}. \tag{51}$$

Figure 1 shows the tricritical bifurcation curves, defined by $\lambda^2/(\phi Da)\,(1-n)f_p^{\,2/(n-1)} = 1/(5\pi^2)$, where a transition from supercritical to subcritical bifurcation may occur, in the (n, λ) plane for different values of the product ϕDa. For a prescribed value of ϕDa, the bifurcation is supercritical below the tricritical bifurcation curve, becoming subcritical otherwise. We can see in Fig. 1 that when the index n approaches $n = 1$, the curves go to infinity, attesting a supercritical bifurcation for all values of ϕDa as in the case of a Newtonian fluid. However, this figure also shows that decreasing n, which means more shear-thinning effects, promotes a subcritical bifurcation. The same conclusion can be drawn if the characteristic time of the fluid λ is increased. On the other hand, this figure indicates that more permeable porous materials may promote a supercritical nature of the bifurcation.

For laboratory experiments, one needs realistic values to properly interpret the bifurcation diagram shown in Fig. 1. Expression (51) may be written in dimensional form as,

$$\phi K < (\phi K)^{tr} = 5\,\pi^2\,(1-n)f_p^{\frac{2}{n-1}}\,\lambda^{*2}\,\frac{\kappa_m^2}{H^2} \tag{52}$$

where $(\phi K)^{tr}$ is the particular value of the product of the porosity and the permeability needed for the observability of a subcritical bifurcation. For real pseudoplastic fluids,

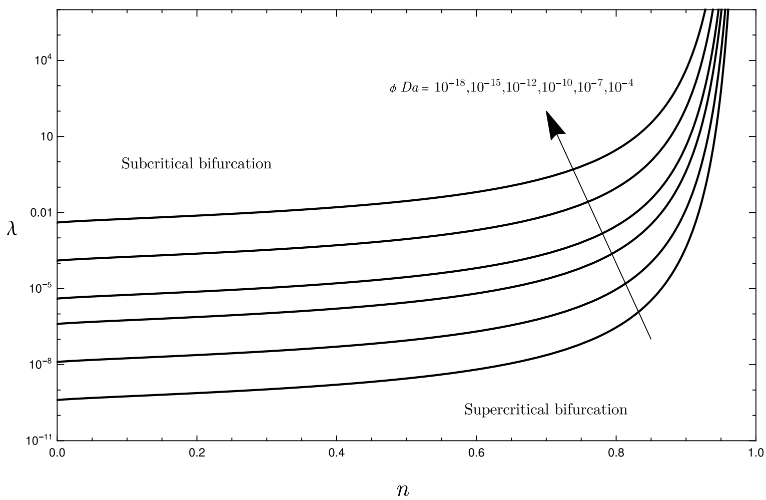

Fig. 1 Tricritical bifurcation curves separating regions of subcritical and supercritial bifurcation in (n, λ) plane at different values of ϕDa corresponding to pseudoplastic fluids

the time characteristic of the fluid λ^* may vary from 0.1 to 100 s. If we fix the height of the porous cavity to $H = 4 \times 10^{-2}$ m, the thermal diffusivity of the medium to $\kappa_m = 10^{-7}\,\mathrm{m}^2\,\mathrm{s}^{-1}$ and the power index to $n = 0.5$, then $(\phi K)^{tr}$ may vary from $10^{-12}\,\mathrm{m}^2$ to $10^{-6}\,\mathrm{m}^2$. As for common porous materials, the values of the permeability K vary widely from $10^{-20}\,\mathrm{m}^2$ to $10^{-7}\,\mathrm{m}^2$ while a typical value of the porosity ϕ is 0.35, the subcritical bifurcation from conductive state to convection rolls predicted by the present weakly nonlinear stability analysis may be effective in laboratory experiments for realistic parameters.

It is instructive to point out that the transition to a subcritical bifurcation in convection problems was also predicted for non-Newtonian fluids different from pseudoplastic fluids. Balmforth and Rust (2009) performed a weakly nonlinear stability analysis of viscoplastic fluid convection and showed that sufficient shear thinning can make the transition to instability subcritical. Recently and for the first time, Rees (2020) used a weakly nonlinear theory together with numerical simulations to study the Bingham fluids convection in a porous medium. By adopting the regularized Pascal model, Rees (2020) showed that convection first appears as a strongly convecting motion via a subcritical bifurcation.

3.3 Equilibrium Amplitude, Isocontours and Average Heat Transfer

The amplitude equation (46) predicts supercritical instability for dilatant fluids, independent of the parameter α_p, and also for pseudoplastic fluids, if $\alpha_p < \alpha_p^{tr}$, both yielding the stable stationary nonlinear equilibrium solution,

$$\begin{aligned} |A_s| &= \left[\frac{Ra - Ra_c}{Ra_c}\right]^{1/2} \frac{1}{\pi} \frac{1}{\left(1 \pm 10\,\pi^2\,\alpha_p\right)^{1/2}} \\ &= \frac{|A_s^N|}{\left(1 \pm 10\,\pi^2\,\alpha_p\right)^{1/2}} \end{aligned} \tag{53}$$

where the + and − signs correspond, respectively, to dilatant and pseudoplastic fluids and A_s^N is the equilibrium amplitude for Newtonian fluids defined as,

$$|A_s^N| = \frac{1}{\pi}\left[\frac{Ra - Ra_c}{Ra_c}\right]^{1/2} \tag{54}$$

Figure 2 presents the bifurcation diagram showing the equilibrium amplitude for dilatant ($n > 1$) and pseudoplastic ($n < 1$) fluids when the bifurcation is supercritical. The amplitude is represented as a function of the relative distance to criticality for different values of α_p, varying from 0.1 to 0.6 for pseudoplastic fluids and from 0.2 to 2.2 for dilatant fluids. The dashed, continuous and dotted curves represent the Newtonian, pseudoplastic and dilatant fluid amplitudes, respectively. This figure shows that the pseudoplastic fluid convection amplitude grows as α_p increases and approaches the tricritical point α_p^{tr}. We also observe that convection in pseudoplastic fluids is more vigorous compared to the Newtonian fluid case. Contrary to the pseudoplastic fluids, the dilatant fluid convection amplitude decreases with the bifurcation parameter α_p, i.e., convection is weaker compared to the Newtonian fluid case.

For pseudoplastic fluids, in the parametric region where $\alpha_p > \alpha_p^{tr}$, the bifurcation is subcritical and the cubic amplitude equation (46) does not provide any stable finite-amplitude

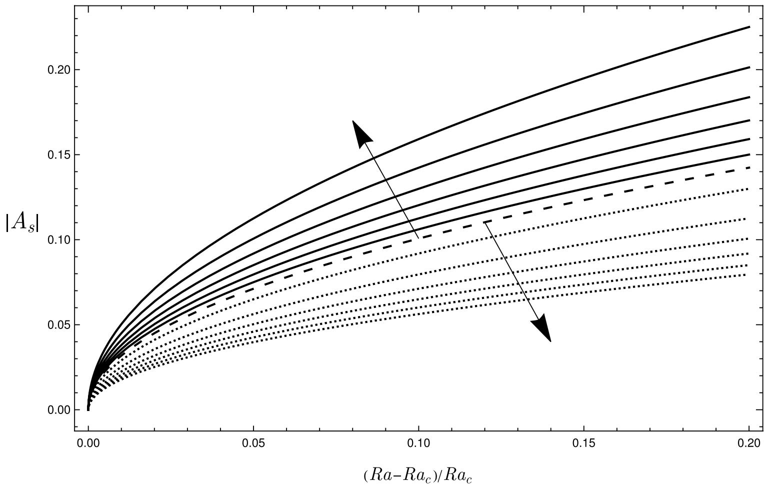

Fig. 2 Finite amplitude of supercritical instability versus the relative distance to criticality. Continuous curves correspond to pseudoplastic fluids, the single dashed curve in the center corresponds to the Newtonian fluid case while the dotted curves below correspond to the dilatant fluids. Starting from the Newtonian curve, α_p varies from 0.1 to 0.6 times α_p^{tr} for pseudoplastic fluids and from 0.2 to 2.2 times α_p^{tr} for dilatant fluids. The arrows indicate the direction in which α_p grows

equilibrium. Therefore, it would be necessary to carry the analysis to higher orders to find such solutions. This task is out of the scope of the present work.

The Nusselt number measures the total vertical heat transfer through the layer induced by convection and conduction reduced by its conductive contribution. The mean Nusselt number N evaluated at $z = 0$, where the vertical velocity vanishes, is defined as

$$N = 1- < \frac{\partial \theta}{\partial z}(z = 0) > \tag{55}$$

where $< \cdot >$ represents an horizontal average over one wavelength of the quantity being averaged. Doing so yields

$$\begin{aligned} Nu - 1 &= \left[\frac{Ra - Ra_c}{Ra_c}\right] \frac{2}{\left(1 \pm 10\,\pi^2\,\alpha_p\right)} \\ &= \frac{(Nu^N - 1)}{\left(1 \pm 10\,\pi^2\,\alpha_p\right)} \end{aligned} \tag{56}$$

where Nu^N is the Nusselt number for Newtonian fluids,

$$Nu^N - 1 = 2\left[\frac{Ra - Ra_c}{Ra_c}\right] \tag{57}$$

which is exactly the same one derived in Joseph (2013).

Figure 3 shows the Nusselt number for pseudoplastic and dilatant fluids as a function of the relative distance to the critical Rayleigh number for different values of the bifurcation parameter α_p. The Newtonian fluid case is also presented for comparison purposes. The dashed, continuous and dotted curves correspond to the Newtonian, pseudoplastic and

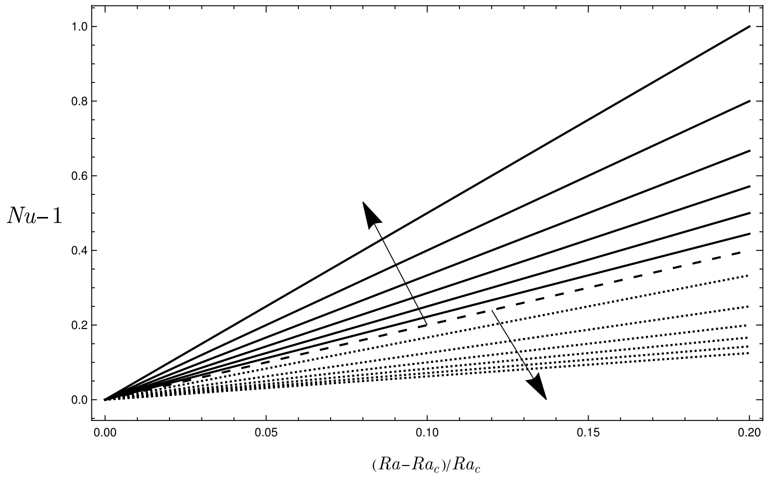

Fig. 3 Convective Nusselt number versus the relative distance to criticality. Continuous curves correspond to pseudoplastic fluids, the single dashed curve in the center corresponds to the Newtonian fluid case while the dotted curves below correspond the dilatant fluids. Starting from the Newtonian curve, α_p varies from 0.1 to 0.6 times α_p^{tr} for pseudoplastic fluids and from 0.2 to 2.2 times α_p^{tr} for dilatant fluids. The arrows indicate the direction in which α_p grows

dilatant fluids, respectively. It is interesting to note that the heat transfer is always higher in a pseudoplastic fluid convection, compared to the Newtonian case. The Nusselt number also increases when α_p increases, as a consequence of the higher amplitude of convection rolls. According to the definition (49) for α_p, this means that heat transfer is higher for strongly shear-thinning fluid and weakly permeable porous material. The opposite trend is observed for dilatant fluids.

The intensity of the streamfunction and temperature fields depend on the relative distance to the critical Rayleigh number and on the value of the bifurcation parameter α_p. Here the prescribed values of these two parameters are, respectively, $\frac{Ra-Ra_c}{Ra_c} = 0.1$ and $\alpha_p = 0.5\,\alpha_p^{tr}$. Figure 4 presents the disturbance isotherms for pseudoplastic fluid,

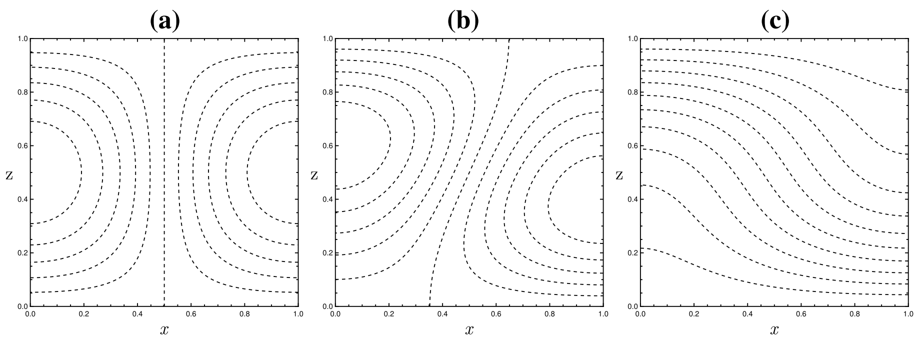

Fig. 4 Disturbance Isotherm patterns for pseudoplastic fluids obtained by linear stability (**a**) and nonlinear stability (**b**). The total temperature field including the conductive state is represented in (**c**). The prescribed parameters are $\frac{Ra-Ra_c}{Ra_c} = 0.1$ and $\alpha_p = 0.5\,\alpha_p^{tr}$

considering a single convective cell in the spatial domain, obtained by linear stability analysis (a), nonlinear stability analysis (b) and the total temperature field (c), including the basic state. As can be seen from Fig. 4b, the nonlinear interaction distorts the linear fundamental mode and breaks the symmetry with respect to the vertical and horizontal midplanes. Figure 5 presents the spatial profile of the convective fields in terms of streamfunction (continuous lines) and the total temperature field (dashed lines) isocontours. The results are shown for pseudoplastic (a) and dilatant (b) fluids. In this figure, the streamlines are seen to be equally spaced between $\psi = 0$, at the horizontal boundaries, and the maximum value at the center of the cell. The thermal structure behaves qualitatively in the same way as in the Newtonian case and consists of hot ascending and cold descending plumes. The results for dilatant fluids are qualitatively similar.

For non-Newtonian fluids, the dimensionless apparent viscosity changes its spatial structure when the convection takes place, contrary to the Newtonian fluid case where it is uniform and equal to one. Figure 6 shows the isolines of apparent viscosity for pseudoplastic (a) and dilatant (b) fluids. As expected, the local apparent viscosity μ_a in the presence of convection is lower than one for pseudoplastic fluids and higher than one for dilatant fluids. Both plots indicate that $\mu_a \approx 1$ near the center of the cell and at the neighborhood of its four corners, as a consequence of nearly vanishing convective velocity in these locations. These plots clearly show that the minimum (maximum) of the apparent viscosity in pseudoplastic (dilatant) fluids occurs in the middle of the horizontal and vertical boundaries of the cell where the absolute value of the convective velocity is at its maximum.

3.4 Apparent Rayleigh Number, Universal Equilibrium Amplitude and Nusselt Number

Parmentier (1978) investigated thermal convection in non-Newtonian dilatants fluids with a power law exponent n in the range $1 < n < 9$. He introduced an apparent Rayleigh

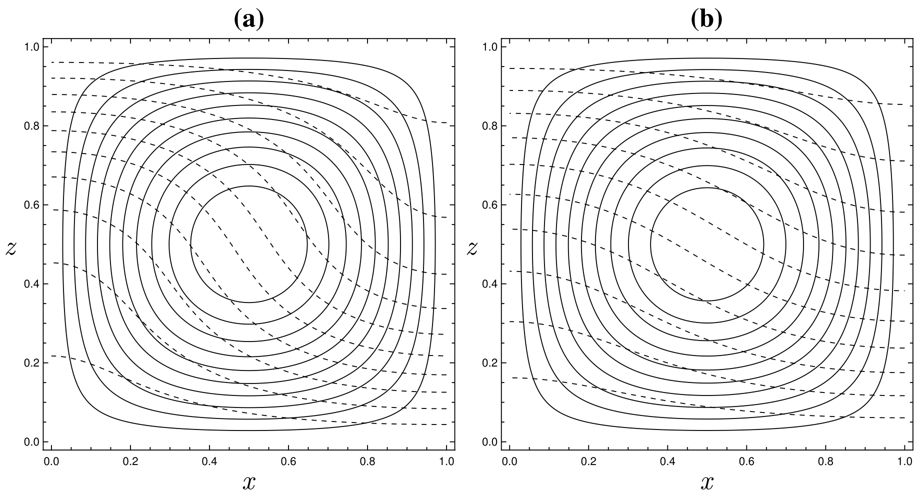

Fig. 5 Streamline and isotherm patterns obtained for pseudoplastic (**a**) and dilatant (**b**) fluids at $\frac{Ra-Ra_c}{Ra_c} = 0.1$ and $\alpha_p = 0.5\,\alpha_p^{tr}$

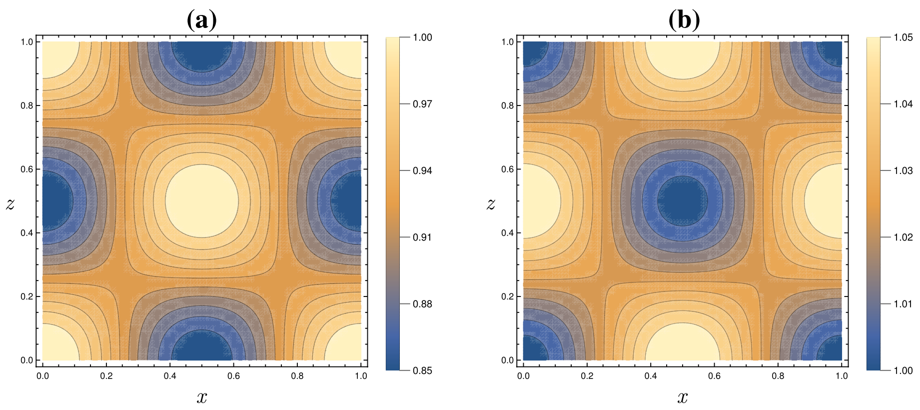

Fig. 6 Apparent viscosity isolines for pseudoplastic (**a**) and dilatant (**b**) fluids at $\frac{Ra-Ra_c}{Ra_c} = 0.1$ and $\alpha_p = 0.5\,\alpha_p^{tr}$

number based on the average viscosity and showed that all different Nusselt number curves for various values of n collapse on the universal curve for a Newtonian fluid. For porous media saturated with non-Newtonian fluids, the average apparent viscosity will be defined by deploying a momentum energy analysis. Multiplying the complex conjugate of u and w to the x and z components of the momentum equation (17), respectively, adding both equations, and integrating the resulting equation along x and z, leads to the expression for the perturbation energy

$$\mathrm{e}_{\mathrm{th}} + \mathrm{e}_{\mathrm{d}} = 0 \tag{58}$$

where the two contributions are given by

$$\mathrm{e}_{\mathrm{th}} = Ra \int_0^1 \int_0^{2\pi/k_c} (w^*\,\theta)\,\mathrm{d}x\,\mathrm{d}z \tag{59}$$

$$\mathrm{e}_{\mathrm{d}} = -\int_0^1 \int_0^{2\pi/k_c} \mu_a\,(|u|^2 + |w|^2)\,\mathrm{d}x\,\mathrm{d}z \tag{60}$$

with $\mu_a = \left(1 \pm \alpha_p\,(|u|^2 + |w|^2)\right)$ and w^* is the complex conjugate of w.

The energy e_{th} corresponds to the thermal buoyancy energy contribution due to the imposed temperature gradient whereas e_{d} corresponds to the viscous dissipation energy.

If we define the average apparent viscosity $\overline{\mu}_a$ as

$$\overline{\mu}_a = \frac{\int_0^1 \int_0^{2\pi/k_c} \mu_a\,(|u|^2 + |w|^2)\,\mathrm{d}x\mathrm{d}z}{\int_0^1 \int_0^{2\pi/k_c}(|u|^2 + |w|^2)\,\mathrm{d}x\mathrm{d}z} \tag{61}$$

equation (58) becomes

$$\overline{Ra} \int_0^1 \int_0^{2\pi/k_c} (\tilde{w}\,\theta)\,\mathrm{d}x\,\mathrm{d}z - \int_0^1 \int_0^{2\pi/k_c} (|u|^2 + |w|^2)\,\mathrm{d}x\,\mathrm{d}z = 0 \tag{62}$$

where $\overline{Ra} = Ra/\overline{\mu}_a$ is the apparent Rayleigh number. It should be emphasized that the energy budget equation (62), written in terms of the apparent Rayleigh number, explicitly depends on neither the fluid parameters n and λ nor the porous material parameters Da and ϕ.

By substituting u and w by $\partial\psi/\partial z$ and $-\partial\psi/\partial x$, respectively, and taking into account the expression for ψ determined above, the following analytical expressions for the average viscosity $\overline{\mu}_a$ and the apparent Rayleigh number $\overline{Ra}$ are obtained,

$$\overline{\mu}_a = \left(1 \pm 10\,\pi^4\,\alpha_p\,|A_s|^2\right) \tag{63}$$

$$Ra = \overline{Ra}\left(1 \pm 10\,\pi^4\,\alpha_p\,|A_s|^2\right) \tag{64}$$

According to the current weakly nonlinear approach, which takes into account first order nonlinearities, the expression (53) for $|A_s|^2$ was obtained.

We now expand Ra and $\overline{Ra}$ in power series of the small parameters $(Ra - Ra_c)$ and $(\overline{Ra} - \overline{Ra}_c)$ by setting $Ra = Ra_c + (Ra - Ra_c)$ and $\overline{Ra} = \overline{Ra}_c + (\overline{Ra} - \overline{Ra}_c)$. Therefore, Eq. (64) yields, respectively, at zeroth and first orders

$$\overline{Ra}_c = Ra_c \tag{65}$$

$$Ra - Ra_c = (1 \pm 10\,\pi^2\,\alpha_p)(\overline{Ra} - \overline{Ra}_c) \tag{66}$$

After inserting the above expressions in equations (53) and (56), the equilibrium amplitude and the Nusselt number may be written as a function of the apparent Rayleigh number as

$$|A_s| = \frac{1}{\pi}\left(\frac{\overline{Ra} - Ra_c}{Ra_c}\right)^{1/2} \tag{67}$$

$$Nu - 1 = 2\left(\frac{\overline{Ra} - Ra_c}{Ra_c}\right) \tag{68}$$

The above results state that, for both pseudoplastic and dilatant fluids, the expressions for the equilibrium amplitude and the Nusselt number are similar to those found for Newtonian fluids in equations (54) and (57), respectively, if we change Ra by $\overline{Ra}$.

4 Conclusion

A novel Darcy–Carreau rheological model for the apparent viscosity of non-Newtonian inelastic fluids flowing through a porous medium was proposed in this paper. This model can be seen as an extension of the well known Carreau model, usually used in a non-Newtonian fluid clear of solid material, to porous media. According to this model, the apparent viscosity expression introduces four dimensionless parameters, namely the power law index n, the characteristic time of the fluid λ, the Darcy number Da and the porosity ϕ of the porous medium. Compared to the classical power law model, the use of this rheological model has major implications, especially in the range of small seepage velocity found at the onset of natural convection. The linear and weakly nonlinear stability analysis of natural convection in porous media saturated by a pseudoplastic fluid ($n < 1$) as well as a dilatant fluid ($n > 1$) is carried out using this Darcy–Carreau model. The linear stability results showed that the critical value of Rayleigh number needed to trigger the thermal instability in non-Newtonian fluids and the corresponding critical wave number are the same as in Newtonian fluids. Although this result is not new for dilatant fluids, since it was originally discovered by Nield (2011a), the present Darcy–Carreau model indicates that it also holds for pseudoplastic fluids.

The nonlinear perturbation behavior has been investigated using weakly nonlinear theory. The coefficients of the appropriate cubic Landau amplitude equation that describes stationary convection rolls beyond instability threshold have been determined. The effect of the two nonlinear terms in the governing equations, namely the advection and non-Newtonian apparent viscosity terms, have been discerned. It is shown that the nonlinear effect depends on a single dimensionless parameter $\alpha_p(n, \lambda, Da, \phi)$, which is proportional to the characteristic time of the fluid λ and is inversely proportional to the properties of the porous medium Da and ϕ. Keeping in mind that increasing the bifurcation parameter α_p means physically increasing the shear-thinning (shear-thickening) character of the pseudoplastic (dilatant) fluid or decreasing the permeability of the porous medium, the main results obtained through this analysis are the following:

- In dilatant fluids, the bifurcation from the conductive state to convection rolls is always supercritical independent of the dimensionless parameter α_p. The amplitude of these rolls and the average convective heat flux decrease with an increase in α_p.
- In pseudoplastic fluids, there exists a tricritical value α_p^{tr}, of the dimensionless parameter α_p, such that a supercritical (subcritical) bifurcation happens when $\alpha_p < \alpha_p^{tr}$ ($\alpha_p > \alpha_p^{tr}$). The physical interpretation of this result lies in the fact that the nonlinear advection term tends to favor a supercritical bifurcation, while the non-Newtonian part in the apparent viscosity promotes a subcritical bifurcation. In the case of a supercritical bifurcation, it was found that the amplitude of convection rolls increases and the average heat flux is enhanced when increasing the parameter α_p, contrary to dilatant fluids.
- The results for both pseudoplastic and dilatant fluids indicate that the equilibrium amplitude of convection and the Nusselt number, when quantified in terms of an apparent Rayleigh number based on the average apparent viscosity, can be successfully described by universal curves that are independent of the rheological parameters and the macroscale properties of the porous medium.

In this paper, we have restricted the analysis to the cubic Landau amplitude equation. However, it would be desirable to go beyond the cubic Landau amplitude equation by considering higher nonlinearities in order to compute the equilibrium amplitude for pseudoplastic fluids with $\alpha_p > \alpha_p^{tr}$, which yields a subcritical bifurcation. This task is under consideration and will be the objective of a future paper.

Recently, Petrolo et al. (2020) investigated theoretically and experimentally the onset of convection under a horizontal throughflow of pseudoplastic fluids in a Hele-Shaw cell. They observed hysteresis effects that may be attributed to the subcritical nature of the bifurcation to mixed convection. For zero basic throughflow, we have shown in the current study that subcritical bifurcation is possible for a known value of the bifurcation parameter α_p. Therefore, it is very interesting to use a nonlinear stability approach to the case when, in addition to the imposed vertical temperature gradient, a horizontal throughflow of pseudoplastic fluids is added. This research is also currently under consideration.

Finally, we want to emphasize that the proposed Darcy–Carreau model of the apparent viscosity in porous media represents a regime of momentum transport that could have potential applications in practical problems qualitatively different from problems involving only thermal instabilities.

Acknowledgements This study was financed in part by the Coordenação de Aperfeiçoamento de Pessoal de Nível Superior - Brasil (CAPES) - Grant n° 88881.174085/2018-01.

Compliance with Ethical Standards

Conflict of interest The authors declare that they have no conflict of interest.

References

Balmforth, N.J., Rust, A.C.: Weakly nonlinear viscoplastic convection. J. Non-Newton. Fluid Mech. **158**, 36–45 (2009)

Barletta, A., Nield, D.A.: Linear instability of the horizontal throughflow in a plane porous layer saturated by a power-law fluid. Phys. Fluids **23**(1), 013102 (2011)

Benouared, O., Mamou, M., Messaoudene, N.A.: Numerical nonlinear analysis of subcritical Rayleigh–Bénard convection in a horizontal confined enclosure filled with non-Newtonian fluids. Phys. Fluids **26**(7), 073101 (2014)

Bouteraa, M., Nouar, C., Plaut, E., Métivier, C., Kalck, A.: Weakly nonlinear analysis of Rayleigh–Bénard convection in shear-thinning fluids: nature of the bifurcation and pattern selection. J. Fluid Mech. **767**, 696–734 (2015)

Carreau, P.J.: Rheological equations from molecular network theories. Trans. Soc. Rheol. **16**(1), 99–127 (1972)

Darbouli, M., Métivier, C., Leclerc, S., Nouar, C., Bouteera, M., Stemmelen, D.: Natural convection in shear-thinning fluids: experimental investigations by MRI. Int. J. Heat Mass Transf. **95**, 742–754 (2016)

Hirata, S.C., Eny, G.E., Ouarzazi, M.N.: Nonlinear pattern selection and heat transfer in thermal convection of a viscoelastic fluid saturating a porous medium. Int. J. Therm. Sci. **95**, 136–146 (2015)

Jenny, M., Plaut, E., Briard, A.: Numerical study of subcritical Rayleigh–Bénard convection rolls in strongly shear-thinning Carreau fluids. J. Non-Newton. Fluid Mech. **219**, 19–34 (2015)

Joseph, D.D.: Stability of Fluid Motions I, vol. 27. Springer, Berlin (2013)

Kim, M.C., Lee, S.B., Kim, S., Chung, B.J.: Thermal instability of viscoelastic fluids in porous media. Int. J. Heat Mass Transf. **46**(26), 5065–5072 (2003)

Kolodner, P.: Oscillatory convection in viscoelastic DNA suspensions. J. non-Newton. Fluid Mech. **75**(2–3), 167–192 (1998)

Liang, S.F., Acrivos, A.: Experiments on buoyancy driven convection in non-Newtonian fluid. Rheol. Acta **9**(3), 447–455 (1970)

Longo, S., Di Federico, V., Chiapponi, L., Archetti, R.: Experimental verification of power-law non-Newtonian axisymmetric porous gravity currents. J. Fluid Mech. **731**, R2 (2013)

Newell, A.C., Whitehead, J.A.: Finite bandwidth, finite amplitude convection. J. Fluid Mech. **38**(2), 279–303 (1969)

Nield, D.A.: A further note on the onset of convection in a layer of a porous medium saturated by a non-Newtonian fluid of power-law type. Trans. Porous Media **88**(2), 187–191 (2011a)

Nield, D.A.: A note on the onset of convection in a layer of a porous medium saturated by a non-Newtonian nanofluid of power-law type. Trans. Porous Media **87**(1), 121–123 (2011b)

Nield, D.A., Bejan, A.: Convection in Porous Media, 5th edn. Springer, Berlin (2017)

Parmentier, E.M.: A study of thermal convection in non-Newtonian fluids. J. Fluid Mech. **84**(1), 1–11 (1978)

Pascal, J.P., Pascal, H.: Nonlinear effects on some unsteady non-Darcian flows through porous media. Int. J. Non-Linear Mech. **32**(2), 361–376 (1997)

Petrolo, D., Chiapponi, L., Longo, S., Celli, M., Barletta, A., Di Federico, V.: Onset of Darcy–Bénard convection under throughflow of a shear-thinning fluid. J. Fluid Mech. **889**, R2 (2020)

Rees, D.A.S.: Darcy–Bénard–Bingham convection. Phys. Fluids **32**, 084107 (2020)

Requilé, Y., Hirata, S.C., Ouarzazi, M.N., Barletta, A.: Weakly nonlinear analysis of viscous dissipation thermal instability in plane Poiseuille and plane Couette flows. J. Fluid Mech. **886**, A26 (2020)
Savins, J.G.: Non-Newtonian flow through porous media. Ind. Eng. Chem. **61**(10), 18–47 (1969)
Taleb, A., BenHamed, H., Ouarzazi, M.N., Beji, H.: Analytical and numerical analysis of bifurcations in thermal convection of viscoelastic fluids saturating a porous square box. Phys. Fluids **28**(5), 053106 (2016)
Tien, C., Sheng, H., Sun, Z.: Thermal instability of a horizontal layer of non-Newtonian fluid heated from below. Int. J. Heat Mass Transf. **12**(9), 1173–1178 (1969)
Yoon, D., Kim, M.C., Choi, C.K.: The onset of oscillatory convection in a horizontal porous layer saturated with viscoelastic liquid. Trans. Porous Media **55**(3), 275–284 (2004)